Inorganic Chemistry

Article

pubs.acs.org/IC

Mild, Reversible Reaction of Iridium(III) Amido Complexes with Carbon Dioxide

Graham E. Dobereiner,[†] Jianguo Wu,[†] Michael G. Manas,[†] Nathan D. Schley,[†] Michael K. Takase,[†] Robert H. Crabtree,*[,†] Nilay Hazari,*[,†] Feliu Maseras,[‡,§] and Ainara Nova*[,‡]

[†]Department of Chemistry, Yale University, P.O. Box 208107, New Haven, Connecticut, 06520, United States

[‡]Institute of Chemical Research of Catalonia (ICIQ), Ave Països Catalans, 16, 43007 Tarragona, Spain

[§]Departament de Química, Universitat Autònoma de Barcelona, 08193 Bellaterra, Spain

Supporting Information

ABSTRACT: Unlike some other Ir(III) hydrides, the aminopyridine complex [(2-NH_2−C_5NH_4)$IrH_3(PPh_3)_2$] (**1-PPh$_3$**) does not insert CO_2 into the Ir−H bond. Instead **1-PPh$_3$** loses H_2 to form the cyclometalated species [(κ^2-*N*,*N*-2-NH-C_5NH_4)$IrH_2(PPh_3)_2$] (**2-PPh$_3$**), which subsequently reacts with CO_2 to form the carbamato species [(κ^2-*O*,*N*-2-OC(O)NH-C_5NH_4)$IrH_2(PPh_3)_2$] (**10-PPh$_3$**). To study the insertion of CO_2 into the Ir−N bond of the cyclometalated species, a family of compounds of the type [(κ^2-*N*,*N*-2-NR-C_5NH_4)$IrH_2(PR'_3)_2$] (R = H, R′ = Ph (**2-PPh$_3$**); R = H, R′ = Cy (**2-PCy$_3$**); R = Me, R′ = Ph (**4-PPh$_3$**); R = Ph, R′ = Ph (**5-PPh$_3$**); R = Ph, R′ = Cy (**5-PCy$_3$**)) and the pyrimidine complex [(κ^2-*N*,*N*-2-NH-$C_4N_2H_3$)$IrH_2(PPh_3)_2$] (**6-PPh$_3$**) were prepared. The rate of CO_2 insertion is faster for the more nucleophilic amides. DFT studies suggest that the mechanism of insertion involves initial nucleophilic attack of the nitrogen lone pair of the amide on CO_2 to form an *N*-bound carbamato complex, followed by rearrangement to the *O*-bound species. CO_2 insertion into **1-PPh$_3$** is reversible in the presence of H_2 and treatment of **10-PPh$_3$** with H_2 regenerates **1-PPh$_3$**, along with $Ir(PPh_3)_2H_5$.

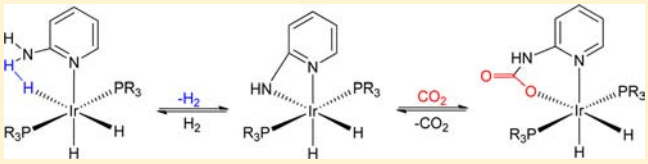

INTRODUCTION

The catalytic conversion of CO_2 to useful products is attractive owing to its widespread availability, low cost, and nontoxic nature.[1] Desirable products include liquid fuels,[2] cyclic carbonates,[3] and formic acid.[4] CO_2 is reactive toward strong nucleophiles (e.g., RMgBr and RLi) but in general reactions with weaker nucleophiles require harsh conditions and more effective catalysts still need to be developed. The insertion of CO_2 into M−X bonds is a crucial step in many catalytic cycles for CO_2 conversion and has been studied in various contexts, including CO_2 hydrogenation[4] and C−C bond formation.[5] These examples of organometallic reactivity differ considerably from those demonstrated in the organic literature.

One well-studied organic example is the reversible reaction of CO_2 with amines to form carbamic acids, where the resulting acids must be "trapped" with base as the carbamate anion in order to isolate any product.[6] Indeed, amines find use in current industrial applications for the "scrubbing" or removal of CO_2 from gaseous waste streams.[7] Far less studied are the analogous reactions with amido complexes to form products containing carbamato ligands. Reactions with metal amido species to form metal carbamato complexes are known,[8] particularly for the early transition metals, but there are only scattered reports for the platinum group metals, and few mechanistic details have been determined for these reactions. Furthermore, the majority of these examples feature *N*,*N*-dialkylcarbamato ligands because of the relative solubility of the resulting compounds and few monosubstituted complexes are known.[9]

A rare example involving a monosubstituted amido and a platinum group metal was reported by Bergman and Andersen,[10] who found that a ruthenium amido complex underwent facile reaction with CO_2 to form a carbamato complex (Scheme 1a). This reaction occurred without prior ligand dissociation, and based on observations from low temperature NMR spectroscopy, it was postulated that the reaction involved direct electrophilic attack of CO_2 by the nitrogen atom to form an *N*-bound carbamato species, which would rearrange to form the final *O*-bound product. The feasibility of this mechanism was established when Roundhill demonstrated that an isolated Pt *N*-bound carbamato complex, generated from CO_2 and a Pt amido species, readily rearranged to the *O*-bound product in a polar solvent (Scheme 1b).[11] Early in 2012, we demonstrated that a Ni amido species supported by a PCP pincer ligand (PCP = bis-2,6-ditert-butylphosphinomethylbenzene) also undergoes CO_2 insertion via a mechanism that involves nucleophilic attack of the amide on CO_2 followed by rearrangement from an *N*-bound carbamato complex to an *O*-bound carbamato complex (Scheme 1c).[12]

In a recent computational study[13] we compared the relative hydricity of iridium(III) hydrides and used this information to

Received: May 6, 2012
Published: August 28, 2012

Scheme 1. (a) Reaction of a Ru Amido Complex with CO_2,[10] (b) Reaction of a Pt Amido Complex with CO_2,[11] (c) Reaction of a Ni Amido Complex with CO_2[12]

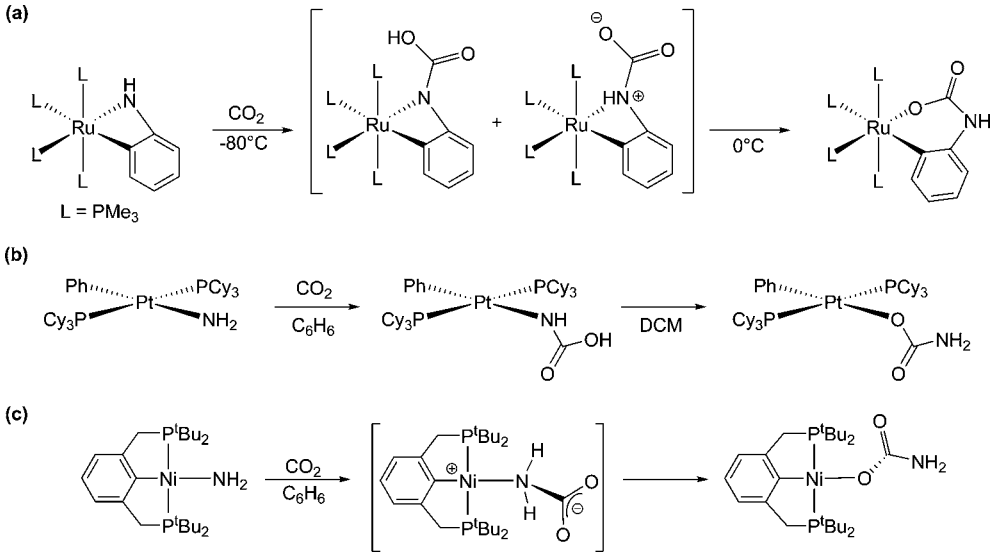

build a model to predict the relative thermodynamic favorability of insertion of CO_2 into the Ir−H bond, a proposed mechanistic step in the hydrogenation of CO_2.[14] We developed a highly active CO_2 hydrogenation catalyst with an N−H hydrogen bond donor in the secondary coordination sphere (Figure 1a); this N−H improved the thermodynamic favorability of CO_2 insertion. As a continuation of this investigation we were interested in the reactivity of CO_2 with other iridium(III) hydrides having H-bond donors in the secondary coordination sphere.

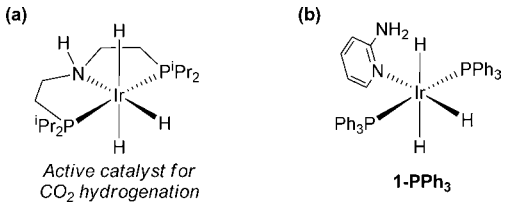

Figure 1. (a) Our prior catalyst for CO_2 hydrogenation.[13] (b) A related pendant amine compound.[15].

We previously reported a *mer* iridium trihydride complex **1-PPh$_3$** (Figure 1b)[15] in the context of the H···H dihydrogen bonding between an Ir−H and the N−H proton of the 2-aminopyridine ligand. This complex was found to lose an equivalent of H_2 thermally to generate an iridium amido species. Here, we report that **1-PPh$_3$** reacts with CO_2 to form a carbamato complex, rather than the expected formate complex. The reaction proceeds via initial H_2 loss, followed by insertion of CO_2 into the Ir−N bond of the cyclometalated species. Moreover, in some cases the CO_2 can be liberated upon treatment of the carbamato complex with H_2 to regenerate the iridium starting material. We have investigated the CO_2 insertion in detail from DFT calculations and a structure−activity study using a family of related Ir complexes.

■ RESULTS AND DISCUSSION

Synthesis of Iridium Amido Complexes. Our previous study of **1-PPh$_3$** revealed that spontaneous loss of H_2 under ambient conditions generated the iridium amido complex, **2-PPh$_3$**;[15] however, this product was not isolated or fully characterized at that time. We have now developed a viable synthesis for **2-PPh$_3$** (Scheme 2) and have fully characterized this species. Complex **3-PPh$_3$**, formed by treatment of $[IrH_2(THF)_2(PPh_3)_2]BF_4$[16] with 2-aminopyridine, can be deprotonated by 1,8-diazabicyclo[5.4.0]undec-7-ene (DBU)

Scheme 2. Synthesis of 1-PPh$_3$ or 2-PPh$_3$ from a Single Cationic Intermediate 3-PPh$_3$

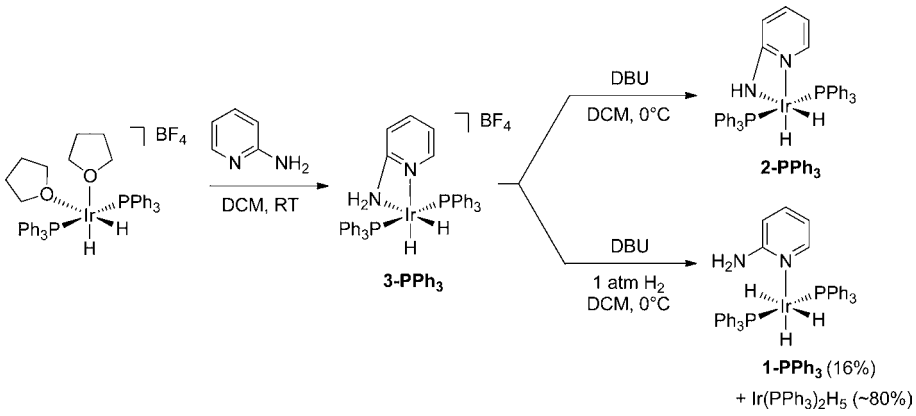

dx.doi.org/10.1021/ic300923c | Inorg. Chem. 2012, 51, 9683−9693

to generate **2-PPh$_3$**. If the deprotonation takes place under an H_2 atmosphere, **1-PPh$_3$** is formed, along with $Ir(PPh_3)_2H_5$.[17] In a typical experiment using 1 atm of H_2 only around 16% of **1-PPh$_3$** is formed but the selectivity is highly dependent on the exact temperature and pressure.

As part of this study the X-ray structure of **1-PPh$_3$** was elucidated (Figure 2). There is disorder in the position of the pyridyl ligand but it was possible to locate the position of the N−H protons of the major component. One of the N−H protons appears to be forming an H-bond with an Ir−H. Although the hydrides on Ir were found in a difference Fourier map, an unambiguous assignment is impossible due to disorder in the ligands and residual electron density around the Ir center. Nevertheless the crystal structure clearly shows that the coordination sphere around Ir contains two *trans* PPh_3 ligands, three hydrides, and a κ^1-bound aminopyridine.

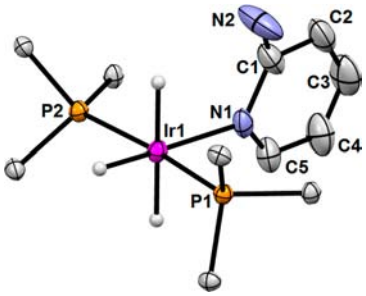

Figure 2. ORTEP of major component of **1-PPh$_3$** at 30% probability. Selected bond lengths (Å) and angles (deg): Ir(1)−P(1) 2.2693(8), Ir(1)−P(2) 2.2638(8), Ir(1)−N(1) 2.208(9), N(1)−C(1) 1.45(4), N(2)−C(1) 1.122(15), C(1)−C(2) 1.387(19), C(2)−C(3) 1.365(16), C(3)−C(4) 1.322(15), C(4)−C(5) 1.403(19); P(1)−Ir(1)−P(2) 171.38(3), P(1)−Ir(1)−N(1) 92.7(11), P(2)−Ir(1)−N(1) 95.8(11). The phenyl groups of PPh_3 and the disorder in the 2-aminopyridine ligand are hidden for clarity.

The complexes **2-PPh$_3$** (Figure 3a) and **3-PPh$_3$** (Figure 3b) were also characterized by X-ray crystallography. To the best of our knowledge they are the first crystallographically characterized examples of 2-aminopyridine ligands κ^2-coordinated to Ir, although there are many examples both for other transition metals and the lanthanides.[18] The two complexes have very similar overall geometries. For example, **2-PPh$_3$** features a 4-membered chelating ring with an N(1)−Ir(1)−N(2) angle of 59.3(2)°, while the corresponding angle in **3-PPh$_3$** is 60.8(3)°. Unsurprisingly the Ir(1)−N(2) bond length in **2-PPh$_3$**, 2.190(5) Å, is significantly shorter than the Ir(1)−N(2) bond length in **3-PPh$_3$**, 2.284(8) Å, consistent with the ligand changing from neutral L type in **3-PPh$_3$** to anionic X type in **2-PPh$_3$**. However, comparison of the Ir−N bond lengths in **2-PPh$_3$** reveals that the Ir−$N_{pyridine}$ bond length (Ir(1)−N(1) 2.158(4) Å) is shorter than the Ir−N_{amide} bond length (Ir(1)−N(2) 2.190(5) Å). The bond length difference can be rationalized in terms of a contribution from a resonance form in which the negative charge is localized on the pyridyl nitrogen (Figure 4a). This is confirmed by analyzing the bond lengths in the pyridine ring. Two of the C−C bond lengths (C(2)−C(3) 1.322(8) Å and C(4)−C(5) 1.342(9) Å) are significantly shorter than the other C−C bond lengths (C(1)−C(2) 1.392(7) Å and C(3)−C(4) 1.387(9) Å), in agreement with some contribution coming from the iminopyridinato resonance form (see Figure 4). Recently, Kempe and co-workers have speculated that the iminopyridinato resonance form is favored for late transition metals, especially for the heavier homologues of the triads,[18] and our results are consistent with this hypothesis. In **3-PPh$_3$**, where the 2-aminopyridine ligand is neutral, the C−C bond lengths in the pyridine ring are identical (within error) and the Ir−$N_{pyridine}$ bond length (Ir−N1 2.184(8) Å) is significantly shorter than the Ir−N_{amine} bond length (Ir−N1 2.282(8) Å). The anion in **3-PPh$_3$** appears to be

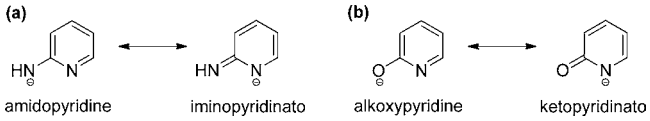

Figure 4. Two limiting resonance forms for deprotonated (a) 2-aminopyridines and (b) 2-hydroxypyridines.

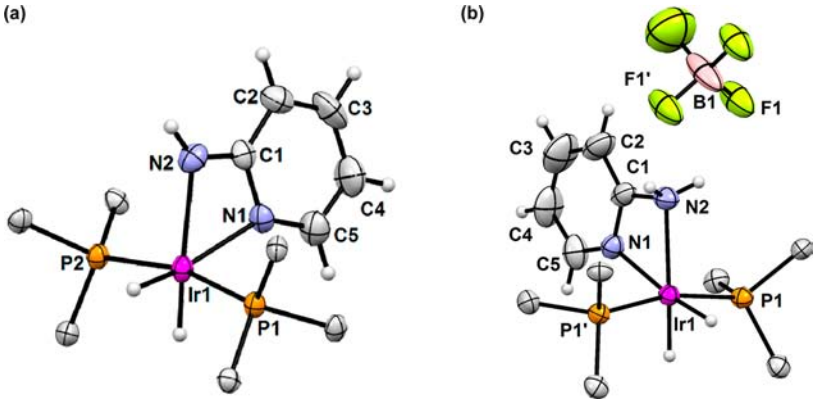

Figure 3. (a) ORTEP of **2-PPh$_3$** at 50% probability. Selected bond lengths (Å) and angles (deg): Ir(1)−P(1) 2.243(1), Ir(1)−P(2) 2.255(1), Ir(1)−N(1) 2.158(4), Ir(1)−N(2) 2.190(5), N(1)−C(1) 1.342(7), N(2)−C(1) 1.303(6), C(1)−C(2) 1.392(7), C(2)−C(3) 1.322(8), C(3)−C(4) 1.387(9), C(4)−C(5) 1.342(9); P(1)−Ir(1)−P(2) 166.51(4), P(1)−Ir(1)−N(1) 92.8(1), P(1)−Ir(1)−N(2) 103.3(1), P(2)−Ir(1)−N(1) 98.0(1), P(2)−Ir(1)−N(2) 89.2(1), N(1)−Ir(1)−N(2) 59.3(2), Ir(1)−N(1)−C(1) 95.9(3). The phenyl groups of PPh_3 are hidden for clarity. (b) ORTEP of **3-PPh$_3$** at 50% probability. Selected bond lengths (Å) and angles (deg): Ir(1)−P(1) 2.295(2), Ir(1)−N(1) 2.184(8), Ir(1)−N(2) 2.282(8), N(1)−C(1) 1.324(12), N(2)−C(1) 1.475(12), C(1)−C(2) 1.364(14), C(2)−C(3) 1.367(19), C(3)−C(4) 1.361(20), C(4)−C(5) 1.366(16); P(1)−Ir(1)−N(1) 93.82(4), P(1)−Ir(1)−N(2) 96.14(4), N(1)−Ir(1)−N(2) 61.1(3), Ir(1)−N(1)−C(1) 99.5(6). The phenyl groups of PPh_3 and the cocrystallized solvent molecules are hidden for clarity.

dx.doi.org/10.1021/ic300923c | *Inorg. Chem.* 2012, 51, 9683−9693

closely associated with the cationic iridium fragment; **3** exhibits two short BF_4···H−N interactions, with a N···F distance of 2.98 Å. A similar interaction has been observed between a BF_4 anion and an NH proton in an Ir(III) complex by Morris and coworkers, although in that case only one H-bond was present.[19]

To assess which factors control reactivity with CO_2, a variety of complexes related to **1-PPh$_3$** and **2-PPh$_3$** were prepared (Figure 5). The PCy_3 analogue of **2-PPh$_3$**, **2-PCy$_3$**, was

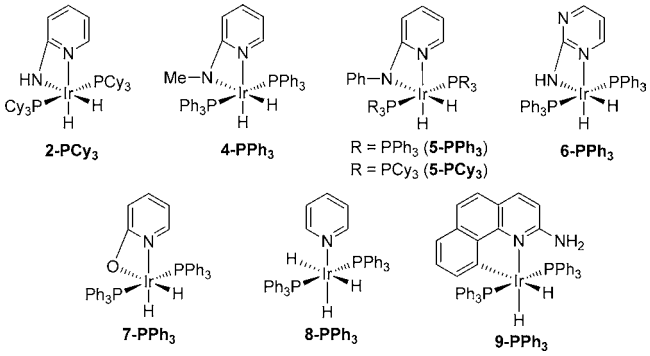

Figure 5. Complexes prepared for screening with CO_2.

synthesized using a different route than the PPh_3 compound, because steric effects preclude the generation of $[(PCy_3)_2(cod)\text{-}Ir]^+$.[20] Instead, the neutral polyhydride $Ir(PCy_3)_2H_5$[21] was treated with 2-aminopyridine at reflux in toluene. This route was also used for the preparation of **5-PCy$_3$**, which contains a 2-*N*-phenylaminopyridine ligand. Similarly, **4-PPh$_3$**, **5-PPh$_3$**, **6-PPh$_3$**, and the previously synthesized compound **7-PPh$_3$**[22] were prepared through the treatment of $Ir(PPh_3)_2H_5$[17] with 2-*N*-methylaminopyridine, 2-*N*-phenylaminopyridine, 2-aminopyrimidine, and 2-hydroxypyridine respectively. The pyridine supported trihydride, **8-PPh$_3$**, which cannot cyclometallate, was prepared through the reaction of pyridine with $Ir(PPh_3)_2H_5$, while the benzo[h]quinoline-2-amine complex **9-PPh$_3$** was prepared through literature methods.[23] All of the new complexes prepared as part of this work were fully characterized.

The complex **7-PPh$_3$** (Figure 6) was characterized by X-ray crystallography. The structure has a geometry nearly identical to that of **2-PPh$_3$** (e.g., N1−Ir1−O1 bond angle of **7-PPh$_3$** is 59.2(2)°, N1−Ir1−N2 angle of **2-PPh$_3$** is 59.3(2)°). The Ir(1)−N(1), 2.169(6), and Ir(1)−O(1), 2.254(4), bond lengths are consistent with those observed in other Ir(III) complexes supported by 2-hydroxypyridyl ligands[24] and suggest some contribution from both the pyridinolato and ketopyridonato resonance form (see Figure 4b). This is again confirmed by analyzing the C−C bond lengths in the pyridine ring. There are two short C−C bonds (C(2)−C(3) 1.358(10) Å and C(4)−C(5) 1.362(10) Å) and two long C−C bonds (C(1)−C(2) 1.404(10) Å and C(3)−C(4) 1.369(9) Å), although the difference is not as pronounced as in **2-PPh$_3$**.

CO_2 Incorporation. The reaction of the trihydride **1-PPh$_3$** with CO_2 in DCM was slow at ambient temperature. Over 24 h, a precipitate formed that was insoluble in most common solvents but sparingly soluble in DCM (Scheme 3). X-ray crystallographic analysis showed that this is the neutral pyridyl carbamato complex, **10-PPh$_3$** (Figure 7a). The carbamato ligand is *O*-bound with an Ir(1)−O(1) bond length of 2.165(3) Å. The Ir(1)−N(1) bond length is 2.126(4) Å, which means that both the Ir−N and Ir−O bonds are shorter than those in

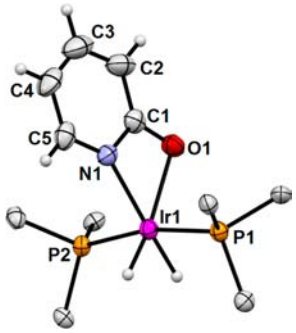

Figure 6. ORTEP of dihydrido(2-hydroxypyridine-κ^2-*O,N*)bis(triphenylphosphine)iridium(III) (**7-PPh$_3$**) at 50% probability. Selected bond lengths (Å) and angles (deg): Ir(1)−P(1) 2.281(1), Ir(1)−P(2) 2.284(1), Ir(1)−O(1) 2.254(4), Ir(1)−N(1) 2.169(6), O(1)−C(1) 1.283(7), N(1)−C(1) 1.337(7), C(1)−C(2) 1.404(10), C(2)−C(3) 1.358(10), C(3)−C(4) 1.369(9), C(4)−C(5) 1.362(10); P(1)−Ir(1)−P(2) 168.19(5), P(1)−Ir(1)−O(1) 93.5(1), P(1)−Ir(1)−N(1) 99.1(1), P(2)−Ir(1)−O(1) 96.0(1), P(2)−Ir(1)−N(1) 91.8(1), O(1)−Ir(1)−N(1) 59.2(2), Ir(1)−O(1)−C(1) 92.5(3). The phenyl groups of PPh_3 are hidden for clarity.

Scheme 3. Proposed Pathway for the Generation of the Carbamato Complex 10-PPh$_3$

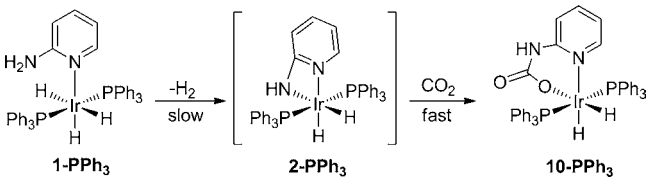

7-PPh$_3$. This is presumably because there is significantly less strain associated with the 6-membered metallacyclic ring in **10-PPh$_3$**, compared with the 4-membered metallacyclic ring in **7-PPh$_3$**. The phosphine ligands are *trans* to one another, and the hydride ligands are mutually *cis*, consistent with the ^{1}H NMR couplings observed for the hydride resonances (triplets of doublets at δ −20.67, J = 16.8, 7.1 Hz, and δ −26.41 J = 17.1, 7.4 Hz). The crystal lattice of **10-PPh$_3$** reveals an intermolecular hydrogen bonding interaction that involves a six membered ring composed of two N−H···O hydrogen bonds with an N···O distance of 2.82 Å (Figure 7b).

A net loss of H_2 must occur in order to form **10-PPh$_3$** from **1-PPh$_3$**. Given that spontaneous loss of H_2 from **1-PPh$_3$** to **2-PPh$_3$** has previously been observed,[15] we hypothesized that **2-PPh$_3$** is the true active intermediate which reacts with CO_2 (Scheme 3). The reaction of a DCM solution of isolated **2-PPh$_3$** with CO_2 resulted in the immediate formation of a precipitate identified as **10-PPh$_3$**, and the reaction appeared to be complete in less than 5 min at room temperature. This indicates that **2-PPh$_3$** is a plausible intermediate. It also suggests that if **2-PPh$_3$** is an intermediate, then the rate determining step in the reaction of **1-PPh$_3$** with CO_2 is the loss of H_2, which is consistent with the observation that **2-PPh$_3$** is not seen as an intermediate by ^{1}H or ^{31}P NMR spectroscopy in the reaction of **1-PPh$_3$** with CO_2. Further support for an initial cyclometalation with formation of an Ir amide came from the lack of reactivity of CO_2 with **9-PPh$_3$**. Due to geometric constraints **9-PPh$_3$** cannot cyclometallate[25] and even at elevated temperatures no reaction was observed between **9-PPh$_3$** and CO_2. An alternative pathway for the formation of **10-PPh$_3$** from **1-PPh$_3$** and CO_2 involves initial insertion of CO_2 into a hydride of **1-PPh$_3$**,

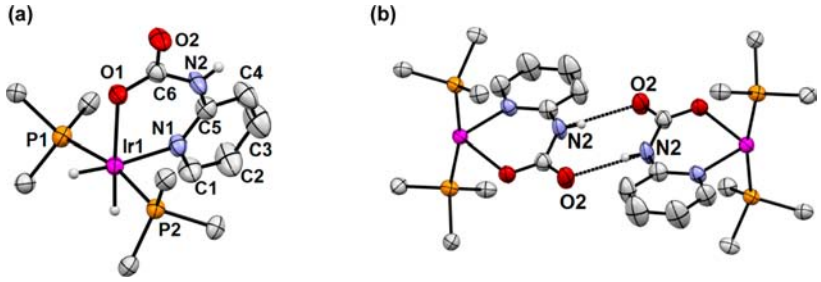

Figure 7. (a) ORTEP of **10-PPh$_3$** at 50% probability. Selected bond lengths (Å) and angles (deg): Ir(1)−P(1) 2.275(2), Ir(1)−P(2) 2.271(2), Ir(1)−O(1) 2.165(3), Ir(1)−N(1) 2.126(4), O(1)−C(6) 1.254(5), O(2)−C(6) 1.231(7), N(2)−C(6) 1.391(7); P(1)−Ir(1)−P(2) 167.38(5), P(1)−Ir(1)−O(1) 90.4(1), P(1)−Ir(1)−N(1) 95.1(1), P(2)−Ir(1)−O(1) 98.6(1), P(2)−Ir(1)−N(1) 94.2(1), O(1)−Ir(1)−N(1) 87.1(2), O(1)−C(6)−O(2) 124.0(5), O(1)−C(6)−N(2) 119.2(5), O(2)−C(6)−N(2) 116.8(5). Selected hydrogen atoms and the phenyl groups of PPh$_3$ are hidden for clarity. (b) Solid state hydrogen bonding interaction in **10-PPh$_3$** between two units in the crystal lattice. The N(2)−O(2) bond length is 2.815 Å. Selected hydrogen atoms and the phenyl groups of PPh$_3$ have been removed for clarity.

followed by H_2 loss. Given our previous studies on the difficulty of CO_2 insertion into Ir(III) hydrides[13] and the fact that the control compound **8-PPh$_3$** (which cannot form a carbamato complex) does not react with CO_2, this route seems unlikely.

To further understand the factors controlling the reactivity of the amido species with CO_2, all of the cyclometalated complexes prepared as part of this work were exposed to CO_2 in DCM. The results are summarized in Table 1. Several of our amido complexes react with CO_2 to form carbamato complexes, analogous to **2-PPh$_3$**. The PCy$_3$ complex, **2-PCy$_3$**, and a N−Me species, **4-PPh$_3$**, undergo facile reaction with CO_2 under ambient conditions to form **10-PCy$_3$** and **11-PPh$_3$**, respectively. The reactivity of **4-PPh$_3$** demonstrates that CO_2 incorporation is not dependent on the presence of an N−H proton. However, in this case complete conversion of **4-PPh$_3$** to **11-PPh$_3$** was not observed and under 1 atm of CO_2 at room temperature a 9:1 mixture of product to starting material was present. Furthermore, the product **11-PPh$_3$** could not be isolated on a reasonable scale, as exposure to vacuum resulted in the loss of CO_2 and the regeneration of **4-PPh$_3$**. It was possible to grow crystals of **11-PPh$_3$** for X-ray diffraction under an atmosphere of CO_2 (vide infra) but exposure of these crystals to vacuum resulted in loss of CO_2. In contrast to these rapid reactions, the reaction between the pyrimidine complex **6-PPh$_3$** and CO_2 took several hours at room temperature, and we suggest that this reaction is slower as a result of electronic effects.

Table 1. Reactivity of Cyclometalated Ir Amides with 1 atm CO_2 in DCM

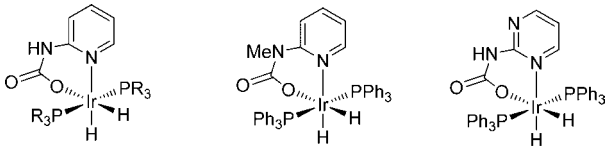

compound	reactivity with CO_2
2-PPh$_3$	instant reaction at room temperature (product **10-PPh$_3$**)
2-PCy$_3$	instant reaction at room temperature (product **10-PCy$_3$**)
3-PPh$_3$	no reaction
4-PPh$_3$	instant reaction at room temperature to give a 9:1 mixture of product and starting material (product **11-PPh$_3$**)
5-PPh$_3$	no reaction
5-PCy$_3$	no reaction
6-PPh$_3$	slow reaction at room temperature (product **12-PPh$_3$**)
7-PPh$_3$	no reaction

Other complexes tried were completely unreactive under ambient conditions. The *N*-phenyl analogues **5-PPh$_3$** and **5-PCy$_3$** are totally unreactive toward CO_2, as is the charged complex **3-PPh$_3$**, which contains a cyclometalated amine ligand rather than a cyclometalated amide ligand. The 2-hydroxypyridyl supported species **7-PPh$_3$** also does not react with CO_2, despite its structural similarities with **2-PPh$_3$**.

The complexes **10-PCy$_3$** and **11-PPh$_3$** were characterized by X-ray crystallography (Figure 8). The structure of **10-PCy$_3$** is analogous to **10-PPh$_3$**, although presumably due to steric factors, the Ir−P bond lengths are longer in **10-PCy$_3$** (Ir(1)−P(1) = 2.3123(16) and Ir(1)−P(2) = 2.3259(16)) compared with **10-PPh$_3$** (Ir(1)−P(1) = 2.275(2) and Ir(1)−P(2) = 2.271(2)). In a comparable fashion to **10-PPh$_3$** two intramolecular N−H···O hydrogen bonding interactions are present in **10-PCy$_3$** to form a dimer (as shown for **10-PPh$_3$** in Figure

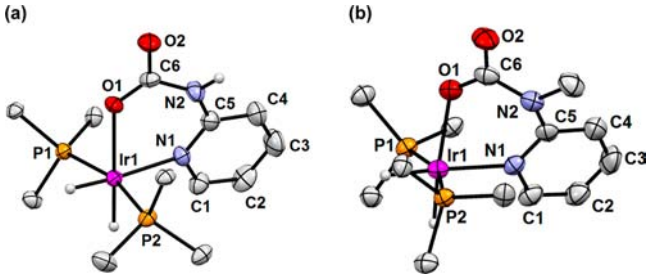

Figure 8. (a) ORTEP of **10-PCy$_3$** at 50% probability. Selected bond lengths (Å) and angles (deg): Ir(1)−P(1) 2.3123(16), Ir(1)−P(2) 2.3259(16), Ir(1)−O(1) 2.198(3), Ir(1)−N(2) 2.189(5), O(1)−C(1) 1.253(7), O(2)−C(1) 1.251(6), N(2)−C(1) 1.401(8); P(1)−Ir(1)−P(2) 164.83(6), P(1)−Ir(1)−O(1) 88.25(11), P(1)−Ir(1)−N(1) 97.08(14), P(2)−Ir(1)−O(1) 98.42(11), P(2)−Ir(1)−N(1) 97.15(14), O(1)−Ir(1)−N(1) 84.24(15), O(1)−C(1)−O(2) 124.7(6), O(1)−C(1)−N(2) 120.8(4), O(2)−C(1)−N(2) 114.5(5). Selected hydrogen atoms and the cyclohexyl groups of PCy$_3$ are hidden for clarity. (b) ORTEP of **11-PPh$_3$** at 50% probability. Ir(1)−P(1) 2.271(2), Ir(1)−P(2) 2.265(2), Ir(1)−O(1) 2.168(5), Ir(1)−N(1) 2.123(4), O(1)−C(6) 1.259(10), O(2)−C(6) 1.222(10), N(2)−C(6) 1.396(8); P(1)−Ir(1)−P(2) 162.37(5), P(1)−Ir(1)−O(1) 98.56(16), P(1)−Ir(1)−N(1) 101.07(18), P(2)−Ir(1)−O(1) 88.05(16), P(2)−Ir(1)−N(1) 96.09(19), O(1)−Ir(1)−N(1) 80.75(17), O(1)−C(6)−O(2) 124.2(6), O(1)−C(6)−N(2) 119.3(7), O(2)−C(6)−N(2) 116.5(7). Selected hydrogen atoms and the phenyl groups of PPh$_3$ are hidden for clarity.

7b). The N···O bond distance is 2.89 Å. In contrast **11-PPh$_3$** does not contain any N−H bonds, and no solid state intramolecular hydrogen bonding is apparent. This may explain why CO_2 insertion into **4-PPh$_3$** does not appear to be as thermodynamically favorable as insertion into **2-PPh$_3$** or **2-PCy$_3$**. In other regards the structure of **11-PPh$_3$** is similar to **10-PPh$_3$**.

Computational Studies of the Mechanism of CO_2 Insertion into 1-PPh$_3$ and Cyclometalated Ir Species. To understand the pathway for CO_2 insertion into **1-PPh$_3$**, a computational study was performed. A model system where PPh_3 was replaced by PH_3 was utilized. The validity of this model was confirmed by performing selected calculations with PPh_3 and these are reported in the Supporting Information. The DCM solvent used in the experiments was included in the calculations using a continuum model. Two possibilities were considered: direct reaction of CO_2 with **1-PH$_3$**, and reaction of CO_2 with the intermediate **2-PH$_3$**, which is obtained by H_2 elimination of **1-PH$_3$**.[26]

CO_2 insertion has previously been observed with the complex (PNP)IrH$_3$ (PNP = HN(^{i}Pr$_2$PC$_2$H$_4$)$_2$) shown in Figure 1a and the insertion of CO_2 into an Ir−H bond of **1-PH$_3$** was calculated (see Figure 9).[13] The Gibbs free energy

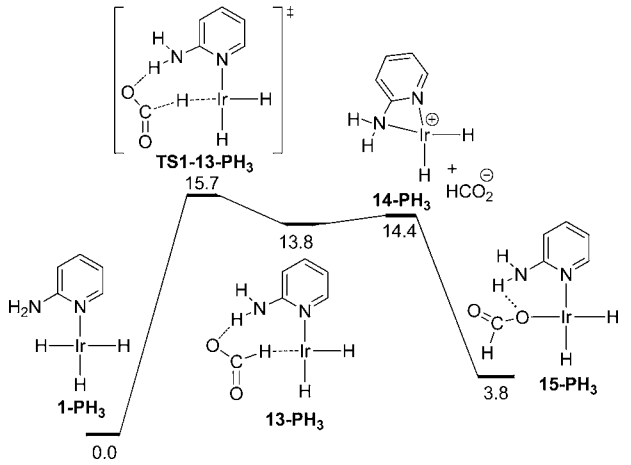

Figure 9. ΔG_{DCM} energy profiles, in kcal mol^{-1}, for CO_2 insertion into Ir−H bond of **1-PH$_3$**. PH_3 ligands have been omitted for clarity.

barrier for CO_2 insertion into one of the *trans* hydrides of **1-PH$_3$** is 15.7 kcal mol^{-1}, which is similar to the energy barrier observed with (PNP)IrH$_3$ (12.4 kcal mol^{-1}). However the reaction with **1-PH$_3$** is slightly endothermic (ΔG_{DCM} = 3.8 kcal mol^{-1}), while it is exothermic (ΔG_{THF} = −4.8 kcal mol^{-1}) using (PNP)IrH$_3$. This is probably a consequence of the lower acidity of the NH$_2$ group compared with the metal bound NH group of (PNP)IrH$_3$, which stabilized the HCO_2^- anion far more effectively through hydrogen bonding. This hypothesis is supported by the higher energy of **14-PH$_3$** + HCO_2^- (ΔG_{DCM} = 14.4 kcal mol^{-1}) compared with the analogous complex with the PNP ligand (ΔG_{THF} = 6.3 kcal mol^{-1}). After formation of **15-PH$_3$**, elimination of H_2 should occur in order to form the final product **10-PH$_3$**. However all the pathways tried were unsuccessful. From **1-PH$_3$**, a pathway where nucleophilic attack of NH$_2$ to CO_2 is concurrent to the H_2 formation was also calculated but it has high energy barriers (see Supporting Information).

The insertion of CO_2 into the NH group of **2-PH$_3$** appears to be a more likely process according to calculation (consistent with our experimental results). Two different pathways were obtained for the insertion: one concerted and the other stepwise (Figure 10). In the concerted mechanism the Ir−O

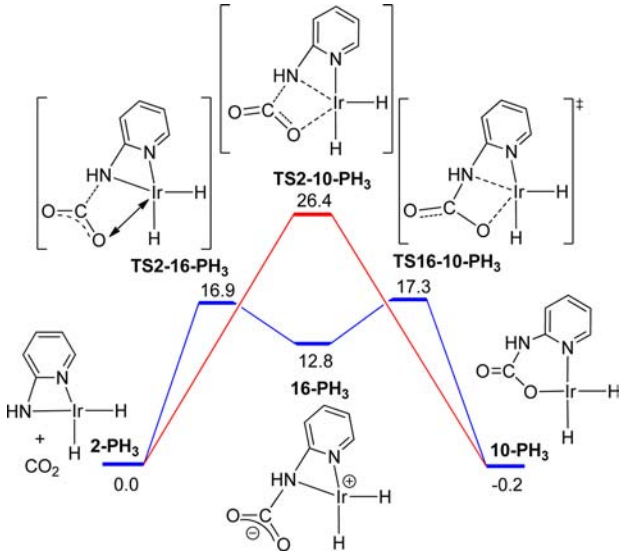

Figure 10. ΔG_{DCM} energy profiles, in kcal mol^{-1}, for the CO_2 insertion into the Ir-NH bond of **2-PH$_3$**. PH_3 ligands have been omitted for clarity.

and N−C bonds are formed simultaneously in **TS2−10-PH$_3$** (Ir···O=2.87 and N···C=2.50 Å), while in the stepwise pathway this happens in two steps. The N−C bond is formed first in **TS2−16-PH$_3$** (N···C=1.95 Å) yielding the *N*-bound carbamato species **16-PH$_3$**. Subsequently, this species undergoes a rearrangement from the *N*-bound to the *O*-bound complex via **TS16−10-PH$_3$** (Ir···N = 2.85 Å, Ir···O = 3.10 Å) to give the final product **10-PH$_3$**.

Comparing the energy barriers for the concerted and stepwise processes, the latter is preferred by 9.1 kcal mol^{-1}. Hence, the stepwise mechanism seems to be the one responsible for the insertion of CO_2 in **2-PH$_3$**. The low Gibbs free energy obtained for the transition states of this process, of 16.9 and 17.3 kcal mol^{-1}, is consistent with a fast reaction of CO_2 with **2-PH$_3$**. This picture also explains why intermediate **2-PPh$_3$** is not observed in the reaction of **1-PPh$_3$** with CO_2, as suggested in Scheme 3. The almost thermoneutral process, with **10-PH$_3$** being only 0.2 kcal mol^{-1} below the reactants (**2-PH$_3$** + **CO$_2$**), is in agreement with a reversible insertion of CO_2 in the absence of hydrogen bonding. Calculations on this mechanism (see Supporting Information) using PPh_3 instead of PH_3 as spectator ligand lead to similar relative energies.

Calculations of the reaction of CO_2 with **4-**, **5-**, and **6-PH$_3$** were also performed in order to check the experimental observations shown in Table 2. The trend observed in the energy barriers of these systems ($\Delta G^{\ddagger}_{DCM}$ = 21.0, 31.1, and 22.3 kcal mol^{-1}, respectively) matches quite well with the experimental results. For instance, the lack of CO_2 insertion with **5-PH$_3$**, using the Py-NPh ligand, is in agreement with a relatively high energy barrier of 31.1 kcal mol^{-1}. In this case the transition state of the stepwise process could not be found, and only a transition state analogous to **TS2−10-PH$_3$** was obtained. This is probably due to the low nucleophilicity of NPh compared to NH and NMe present in the other compounds.

Table 2. Crystal and Refinement Data for Complexes 1-PPh$_3$, 2-PPh$_3$, 3-PPh$_3$, 7-PPh$_3$, 10-PPh$_3$, 10-PCy$_3$, and 11-PPh$_3$

	1-PPh$_3$	2-PPh$_3$	3-PPh$_3$	7-PPh$_3$
empirical formula	$C_{41}H_{39}IrN_2P_2$	$C_{41}H_{37}IrP_2N_2$	$IrP_2N_2BF_4C_{41}H_{38}\cdot1.21\ (CH_2Cl_2)$	$C_{41}H_{36}IrP_2ON$
formula weight	813.88	811.92	1002.50	812.91
temperature (K)	223	223	223	223
a (Å)	11.5834(16)	10.760(7)	19.2265(14)	9.111(4)
b (Å)	12.2221(16)	12.160(7)	15.8767(12)	11.977(6)
c (Å)	13.2838(18)	13.764(9)	15.0485(11)	16.669(7)
α (deg)	90.472(6)	101.791(11)	90	70.480(11)
β (deg)	106.509(7)	94.401(10)	90	81.580(10)
γ (deg)	102.999(7)	111.133(10)	90	73.712(13)
volume (Å^3)	1751.6(4)	1621.9(17)	4593.6(6)	1642.7(13)
Z	2	2	4	2
crystal system	triclinic	triclinic	orthorhombic	triclinic
space group	$P\bar{1}$ (#2)	$P\bar{1}$ (#2)	$Pnma$ (#62)	$P\bar{1}$ (#2)
d_{calc} (Mg/m^3)	1.543	1.866	1.449	1.643
θ range (deg)	3.21−30.51	0.997−27.49	0.996−27.10	0.990−27.48
μ (mm^{-1})	3.934	4.260	3.171	4.208
abs. correction	semiempirical	semiempirical	semiempirical	semiempirical
GOF	1.092	1.095	1.184	1.106
R_1,[a] wR_2[b] [$I > 2\sigma(I)$]	0.0415, 0.0624	0.0411, 0.0657	0.0589, 0.1174	0.0477, 0.0759

	10-PPh$_3$	10-PCy$_3$	11-PPh$_3$
empirical formula	$IrP_2O_2N_2C_{42}H_{37}\cdot2(CH_2Cl_2)$	$IrC_{43}H_{73}O_2N_2P_2\cdot(CH_2Cl_2)$	$IrP_2O_2N_2C_{43}H_{39}\cdot2.5(CH_2Cl_2)$
formula weight	1025.80	977.15	1082.29
temperature (K)	223	223	223
a (Å)	11.729(4)	10.9796(7)	13.269(9)
b (Å)	12.900(5)	12.2163(7)	13.481(8)
c (Å)	15.653(6)	18.3145(13)	14.591(11)
α (deg)	96.745(9)	96.882(7)	66.345(20)
β (deg)	101.430(8)	105.104(7)	71.92(2)
γ (deg)	109.434(8)	102.724(7)	78.945(19)
volume (Å^3)	2145.7(14)	2272.1(3)	2145.7(14)
Z	2	2	2
crystal system	triclinic	triclinic	triclinic
space group	$P\bar{1}$ (#2)	$P\bar{1}$ (#2)	$P\bar{1}$ (#2)
d_{calc} (Mg/m^3)	1.588	1.586	1.586
θ range (deg)	3.25−27.98	3.08−27.16	3.15−27.79
μ (mm^{-1})	3.482	3.170	3.359
abs. correction	semiempirical	semiempirical	semiempirical
GOF	1.089	1.040	1.055
R_1,[a] wR_2[b] [$I > 2\sigma(I)$]	0.0552, 0.0812	0.0541, 0.0922	0.0559, 0.1150

[a] $R_1 = \Sigma||F_o| - |F_c||/\Sigma|F_o|$. [b] $wR_2 = [\Sigma[w(F_o^2 - F_c^2)^2]/\Sigma[w(F_o^2)^2]^{1/2}$.

Calculations on **7-PH$_3$**, a model for the hydroxypyridyl complex **7-PPh$_3$**, reveals that insertion into the Ir−O bond is thermodynamically uphill (ΔG = 17.9 kcal mol^{-1}), which explains the observed lack of reactivity.

Overall, the stepwise mechanism for the CO_2 insertion in **2-PH$_3$** resembles the insertion mechanism observed with the Ru complex shown in Scheme 1a.[10] This process is also similar to the mechanism proposed by our group for the insertion of CO_2 into the Ni−N bound of complex [(PCP)Ni-NH$_2$].[12] However, it should be noted that Chisholm and Extine observed that CO_2 insertion into the W amide bond of W(NMe$_2$)$_6$ and W$_2$(NEt$_2$)$_4$Me$_2$ was catalyzed by fortuitous amine.[27] Elemental analysis suggests that our complexes are pure and do not contain free amine, and the reactions are performed in the absence of water. In addition, the fact that **3-PPh$_3$**, which contains a cyclometalated amine ligand, does not react with CO_2 strongly suggests that a reaction involving a free amine is not occurring.

Reversibility of CO_2 Insertion into 2-PPh$_3$. Treatment of a DCM solution of the carbamato complex **10-PPh$_3$** with ^{13}C-labeled CO_2 produces a significant quantity of the ^{13}C-labeled product over 24 h at room temperature as determined by ^{13}C NMR spectroscopy (Scheme 4). This indicates that the CO_2 insertion is likely a reversible process, and depending on conditions, CO_2 could be liberated.

Scheme 4. Isotopic Exchange of the Carbon Atom in the Carbamato Ligand in 10-PPh$_3$ with $^{13}CO_2$

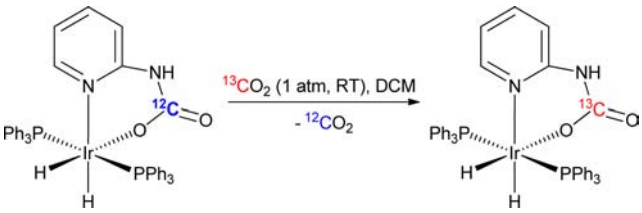

Though complex **10-PPh$_3$** does not lose CO_2 readily at room temperature under vacuum in the solid state (presumably due to the hydrogen bonding), we found that it does react with H_2 even at 1 atm. The reaction of the carbamato complex **10-PPh$_3$** with H_2 at 1 atm and room temperature results in the $Ir(PPh_3)_2H_5$ species within a few hours (Scheme 5). The single hydridic resonance (δ −11.28, triplet, J = 12.0 Hz) present in the ^{1}H NMR spectrum of the reaction mixture indicates that this is the only iridium hydride-containing product.

Scheme 5. Loss of CO_2 from 10-PPh$_3$ under an H_2 Atmosphere to Form $Ir(PPh_3)_2H_5$

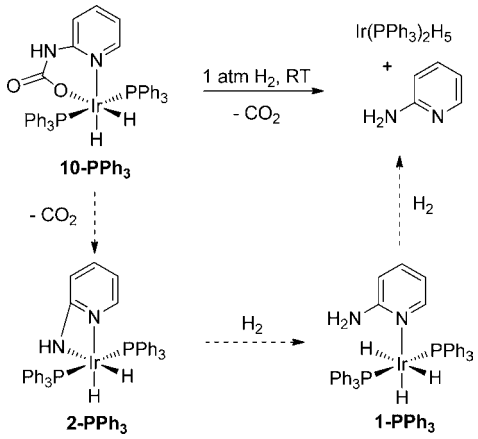

Reaction of complex **1-PPh$_3$** or **2-PPh$_3$** with H_2 at room temperature also results in the formation of $Ir(PPh_3)_2H_5$. Before all of **2-PPh$_3$** is consumed, hydride resonances corresponding to **1-PPh$_3$** are also visible by ^{1}H and ^{31}P NMR spectroscopy, suggesting that **1-PPh$_3$** is an intermediate en route to $Ir(PPh_3)_2H_5$. Peaks corresponding to uncoordinated 2-aminopyridine are also present, confirming the dissociation of the ligand from iridium. Given the reversibility of the CO_2 insertion reaction seen by isotopic labeling, we suggest that **10-PPh$_3$** loses CO_2 to form the Ir amide **2-PPh$_3$**, followed by reaction with two equivalents of H_2 to form $Ir(PPh_3)_2H_5$ (Scheme 5). The hydrogenolysis of **2-PPh$_3$** is likely only possible if the CO_2 incorporation by **10-PPh$_3$** is reversible. H_2 has no obvious role in the release of CO_2, and instead we propose that H_2 serves to trap **2-PPh$_3$** and drive the reaction to completion by the formation of $Ir(PPh_3)_2H_5$, a thermodynamic sink.

■ CONCLUSIONS

CO_2 reacts with an Ir(III) trihydride supported by an 2-aminopyridine ligand, but unlike previous hydrides we have studied,[13] CO_2 does not insert into an Ir−H bond. Instead, the complex undergoes cyclometalation, releasing H_2 and generating a species with an Ir amide bond. This Ir−N bond rapidly inserts CO_2 to form an *O*-bound carbamato complex. The reaction of late transition metal amide bonds with CO_2 has not been extensively studied[10−12] and the factors that promote insertion are still unclear. We have performed an experimental structure−activity study and used calculations to propose a reaction pathway. The reaction proceeds via initial nucleophilic attack of the coordinated amide on CO_2 to form an *N*-bound carbamato species. Ligand rearrangement then occurs to generate the *O*-bound carbamato complex. The rate of reaction depends on the nucleophilicity of the amide, with more nucleophilic amides giving faster rates. The reaction with CO_2 is reversible and addition of H_2 results in the release of CO_2 and the formation of the iridium trihydride. Further work will be needed to find an entry into a potential catalytic cycle that incorporates CO_2 into organic reactants via carboxylation.

■ EXPERIMENTAL SECTION

General. The syntheses of the metal complexes were conducted using standard Schlenk or drybox techniques under a dinitrogen atmosphere using dry, degassed solvents unless otherwise indicated. The solvents for air- and moisture-sensitive reactions were dried by passage through a column of activated alumina followed by storage under dinitrogen. Dihydridobis(tetrahydrofuran) bis(triphenylphosphine)iridium(III) tetrafluoroborate,[16] trihydrido(2-aminopyridine) bis(triphenylphosphine)iridium(III),[15] pentahydridobis(triphenylphosphine)iridium(III),[17] and pentahydridobis(tricyclohexylphosphine)iridium(III)[17] were synthesized according to literature procedures. 2-Aminopyridine was sublimed under high vacuum at room temperature prior to use. All other reagents were purchased commercially from Sigma-Aldrich, Cambridge Isotope Laboratories, Airgas, Alfa-Aesar, or Strem Chemicals and used as received unless otherwise indicated. NMR spectra were recorded at room temperature on a 400 or 500 MHz Bruker or Varian spectrometer. Chemical shifts are reported in ppm with respect to residual internal protio solvent for ^{1}H and ^{13}C{^{1}H} NMR spectra and to an external standard for ^{31}P{^{1}H} spectra (85% H_3PO_4 in H_2O at δ 0.0 ppm). Coupling constants are reported in Hz. IR spectra were measured using diamond smart orbit ATR on a Nicolet 6700 FT-IR instrument unless noted. Elemental analyses were performed by Robertson Microlit Laboratories (Madison, NJ). The ^{1}H and ^{31}P NMR spectra are provided in the Supporting Information for any compounds that did not have satisfactory elemental analyses.

Synthesis and Characterization of Compounds. *Dihydrido(2-amidopyridine-κ^2-N,N′)bis(triphenylphosphine)iridium(III) (2-PPh$_3$).* To a flame-dried Schlenk flask was added dihydrido(2-aminopyridine-κ^2-N,N′)bis(triphenylphosphine)iridium(III) tetrafluoroborate (**3-PPh$_3$**, 200.0 mg, 0.222 mmol, 1.0 equiv) (for preparation of **3-PPh$_3$** see below). The flask was evacuated and backfilled with dinitrogen three times, and 20 mL of dried degassed DCM was added. The reaction was cooled to −30 °C, and a 1 M solution of 1,8-diazabicyclo[5.4.0]undec-7-ene (DBU) in tetrahydrofuran (222 μL, 0.222 mmol, 1.0 equiv) was added dropwise. The reaction was stirred for 30 min, during which time it was allowed to warm to −10 °C and then the solvent was removed under reduced pressure. Ten mL of dried, degassed toluene was added and the resulting suspension was filtered through Celite in vacuo. The filtered solution was evaporated under reduced pressure leaving a light brown residue. This material was recrystallized by layering a concentrated DCM solution with pentane under dinitrogen atmosphere. The solution was decanted off and the solid was dried overnight under vacuum. Crystals suitable for X-ray diffraction were obtained by recrystallization (DCM/pentane, layering, under dinitrogen at RT). Yield 51 mg, 28%. ^{1}H NMR (500 MHz, CD_2Cl_2): δ 7.61−7.55 (m, 12H, PPh$_3$), 7.35−7.23 (m, 18H, PPh$_3$), 6.65 (d, J = 5.3 Hz, 1H, pyridine C−H), 6.52 (t, J = 7.6 Hz, 1H, pyridine C−H), 5.36 (t, J = 6.1 Hz, pyridine C−H), 5.07 (d, J = 8.6 Hz, 1H, pyridine C−H), 3.27 (br s, 1H, −NH), −22.45 to −22.70 (m, 2H, Ir−H). ^{31}P{^{1}H} NMR (202 MHz, CD_2Cl_2): δ 19.42. ^{13}C{^{1}H} NMR (126 MHz, CD_2Cl_2): δ 174.63 (s), 147.32 (s), 136.12 (t, J = 25.4 Hz), 134.77 (t, J = 6.2 Hz), 133.42 (s), 129.82 (s), 128.11 (t, J = 4.8 Hz), 110.23 (s), 103.59 (s). Anal. Calcd for $C_{41}H_{37}IrN_2P_2$: C, 60.65; H, 4.59; N, 3.45. Found: C, 60.41; H, 4.20; N, 3.37.

Dihydrido(2-amidopyridine-κ^2-N,N′)bis(tricyclohexylphosphine)-iridium(III) (2-PCy$_3$). To a suspension of $IrH_5(PCy_3)_2$ (47 mg, 0.06 mmol) in 10 mL of dry C_6H_6 in a 50-mL flame-dried Schlenk flask, 2-aminopyridine (34 mg, 0.36 mmol) was added. The mixture was heated at 75 °C for 37 h. The volatiles were removed under vacuum. The resulting residue was triturated with C_6H_6 (2 × 0.5 mL) to give **2-PCy$_3$** as a white solid, which was dried under vacuum. Yield: 32 mg, 62%. ^{1}H NMR (400 MHz, CD_2Cl_2): δ 7.50 (d, J = 8 Hz, 1H, pyridine

C−H), 6.73 (t, J = 8 Hz, 1H, pyridine C−H), 5.68 (t, J = 8 Hz, pyridine C−H), 5.39 (d, J = 8 Hz, 1H, pyridine C−H), 3.43 (br s, 1H, −NH), 1.80 (br s, 18H) and 1.63 (br s, 12H) and 1.53 (br s, 6H) and 1.28 (m, 12H) and 1.08 (m, 18H) (Cy), −25.37 to −25.66 (m, 2H, Ir−H). $^{31}P\{^1H\}$ NMR (202 MHz, CD_2Cl_2) δ 22.31. $^{13}C\{^1H\}$ NMR (126 MHz, CD_2Cl_2): δ 173.09 (s), 146.69 (s), 133.40 (s), 133.42 (s), 109.55 (s), 100.60 (s), 36.90 (t, J = 13 Hz), 30.59 (br s), 30.51 (br s), 28.47 (br s), 27.48 (s). Anal. Calcd for $C_{41}H_{73}IrN_2P_2{\cdot}CH_2Cl_2$: C, 54.06; H, 8.10; N, 3.00. Found: C, 55.10; H, 8.02; N, 3.17.

Dihydrido(2-aminopyridine-κ²-N,N′)bis(triphenylphosphine)-iridium(III) tetrafluoroborate (3-PPh₃). To a 100-mL flame-dried Schlenk flask was added dihydridobis(tetrahydrofuran) bis-(triphenylphosphine)iridium(III) tetrafluoroborate ($[IrH_2(THF)_2(PPh_3)_2]BF_4$, 914.0 mg, 0.962 mmol). The flask was evacuated and backfilled with dinitrogen three times, and 5 mL of dried degassed DCM was added. A dry degassed solution of 2-aminopyridine (90.4 mg, 0.962 mmol) in DCM (20 mL) was added dropwise over 5 min via cannula transfer. The reaction was allowed to stir for 1.5 h. The yellow solution was concentrated under reduced pressure, resulting in partial precipitation of the product. Fifteen mL of dried degassed diethyl ether was added, and the solution was decanted off the precipitated solid. The solid was washed with diethyl ether (2 × 5 mL) and dried overnight under vacuum. Crystals suitable for X-ray diffraction were grown from DCM/diethyl ether (vapor diffusion, RT). Yield 659.9 mg, 76%. ^1H NMR (500 MHz, CD_2Cl_2): δ 7.59−7.45 (m, 12H, Ar), 7.43−6.98 (m, 20H, Ar), 6.88−6.82 (m, 1H, pyridine C−H), 6.61 (d, J = 8.0 Hz, 1H, pyridine C−H), 3.81 (s, 1H, $-NH_2$), −23.49 (td, J_{PH} = 15.6 Hz, J_{HH} = 8.7 Hz, 1H, Ir−H), −25.32 (td, J_{PH} = 15.8 Hz, J_{HH} = 8.7 Hz, 1H, Ir−H). $^{31}P\{^1H\}$ NMR (202 MHz, CD_2Cl_2): δ 22.48. $^{13}C\{^1H\}$ NMR (126 MHz, CD_2Cl_2): δ 158.03 (s), 148.10 (s), 137.86 (s), 133.37 (t, J = 6.3 Hz), 132.64 (t, J = 26.7 Hz), 130.54 (s), 128.64 (t, J = 5.0 Hz), 124.91 (s), 123.50 (s). Anal. Calcd for $C_{41}H_{38}BF_4IrN_2P_2{\cdot}CH_2Cl_2$: C, 51.23; H, 4.09; N, 2.84. Found: C, 51.65; H, 3.91; N, 2.62.

Trihydrido(2-aminopyridine)bis(triphenylphosphine)iridium(III). An Alternative Preparation from **3**. To a flame-dried Schlenk flask was added dihydrido(2-aminopyridine-κ²-N,N′)bis (triphenylphosphine)iridium(III) tetrafluoroborate (93.7 mg, 0.104 mmol, 1 equiv). After purge and backfill with dinitrogen, a 1 M tetrahydrofuran solution of DBU (115 μL, 0.115 mmol, 1.1 equiv), and 3 mL of DCM were added. The flask was cooled to 0 °C. H_2 was introduced by bubbling and the reaction was stirred for 5 min. The DCM was removed under reduced pressure and 2 mL of toluene was added. The suspension was filtered through Celite under dinitrogen. Degassed pentanes were layered on top of the filtrate and the reaction was stored at −20 °C overnight. The solid was dried in vacuo at 0 °C for 15 min. Yield 13.4 mg, 16%. The spectra of the obtained yellow-white solid were consistent with the previously reported data.[15] $Ir(PPh_3)_2H_5$ is a major byproduct of this reaction and is removed in the filtration step.

Dihydrido(2-methylamidopyridine-κ²-N,N′)bis-(triphenylphosphine)iridium(III) (4-PPh₃). To a suspension of $IrH_5(PPh_3)_2$ (108 mg, 0.15 mmol) in 6 mL of dry C_6H_6 in a 50-mL flame-dried Schlenk flask, 2-methylaminopyridine (16 mg, 0.15 mmol) was added. The mixture was heated at 65 °C for 21 h. The volatiles were removed under vacuum. The resulting residue was recrystallized from a mixture of C_6H_6/pentane (1:3) to give **4-PPh₃** as a pale yellow solid, which was dried under vacuum. Yield: 92 mg, 74%. ^1H NMR (400 MHz, CD_2Cl_2): δ 7.60−7.55 (m, 12H, Ar), 7.36−7.26 (m, 18H, Ar), 6.74 (d, J = 4 Hz, 1H, pyridine C−H), 6.66 (t, J = 8 Hz, 1H, pyridine C−H), 5.25 (m, pyridine C−H), 5.02 (d, J = 8 Hz, 1H, pyridine C−H), 1.80 (s, 3H, −NMe), −22.22 (td, J_{PH} = 16 Hz, J_{HH} = 8 Hz, 1H, Ir−H), −22.75 (td, J_{PH} = 16 Hz, J_{HH} = 8 Hz, 1H, Ir−H). $^{31}P\{^1H\}$ NMR (202 MHz, CD_2Cl_2): δ 20.84 (t, J = 15 Hz). $^{13}C\{^1H\}$ NMR (126 MHz, CD_2Cl_2): δ 171.60 (s), 147.40 (s), 136.14 (t, J = 25 Hz), 133.72 (s), 129.79 (s), 128.88 (s), 128.17 (t, J = 5 Hz), 104.48 (s), 101.55 (s), 32.78 (s). Anal. Calcd for $C_{42}H_{39}IrN_2P_2$: C, 61.08; H, 4.76; N, 3.39. Found: C, 61.33; H, 4.89; N, 3.12.

Dihydrido(2-phenylamidopyridine-κ²-N,N′)bis-(triphenylphosphine)iridium(III) (5-PPh₃). To a suspension of $IrH_5(PPh_3)_2$ (70 mg, 0.10 mmol) in 10 mL of dry C_6H_6 in a 50-mL flame-dried Schlenk flask, 2-phenylaminopyridine (34 mg, 0.20 mmol) was added. The mixture was heated at 65 °C for 25 h. The volatiles were removed under vacuum. The resulting residue was triturated with ether and washed with benzene and dried under vacuum to give **5-PPh₃** as a white solid. Yield: 59 mg, 66%. ^1H NMR (500 MHz, C_6D_6): δ 7.79−7.75 (m, 12H, Ar), 7.01−6.86 (m, 23H, Ar), 6.69 (t, J = 8 Hz, 1H, pyridine C−H), 6.36 (d, J = 10 Hz, 1H, pyridine C−H), 6.19 (d, J = 10 Hz, pyridine C−H), 5.51 (t, J = 6 Hz, 1H, pyridine C−H), −21.61 (td, J_{PH} = 20 Hz, J_{HH} = 10 Hz, 1H, Ir−H), −22.84 (td, J_{PH} = 20 Hz, J_{HH} = 10 Hz, 1H, Ir−H). $^{31}P\{^1H\}$ NMR (202 MHz, C_6D_6): δ 20.67 (t, J = 13 Hz). $^{13}C\{^1H\}$ NMR (126 MHz, C_6D_6) 167.38 (s), 147.81 (s), 147.68 (s), 136.63 (t, J = 25 Hz), 134.63 (t, J = 6 Hz), 129.50 (s), 128.55 (s), 122.47 (s), 121.78 (s), 118.65 (s), 108.66 (s), 106.51 (s). Anal. Calcd for $C_{47}H_{41}IrN_2P_2$: C, 63.57; H, 4.65; N, 3.15. Found: C, 63.32; H, 4.69; N, 3.10.

Dihydrido(2-phenylamidopyridine-κ²-N,N′)bis-(tricyclohexylphosphine)iridium(III) (5-PCy₃). To a suspension of $IrH_5(PCy_3)_2$ (163 mg, 0.21 mmol) in 65 mL of dry CH_2Cl_2 in a 100-mL flame-dried Schlenk flask, 2-phenylaminopyridine (37 mg, 0.21 mmol) was added. The mixture was stirred at RT for 22 h. The volatiles were removed under vacuum. The residue was dissolved in 2 mL of C_6H_6 and a precipitate formed after 10 min. After 1 h the precipitate was collected by filtration, washed with cold CH_2Cl_2, and dried under vacuum. Yield: 89 mg, 46%. ^1H NMR (500 MHz, CD_2Cl_2): δ 7.84 (d, J = 5 Hz, 1H, pyridine C−H), 7.13−7.07 (m, 5H, Ar), 6.64 (t, J = 7 Hz, 1H, pyridine C−H), 6.59 (d, J = 9 Hz, 1H, pyridine C−H), 6.11 (t, J = 7 Hz, 1H, pyridine C−H), 1.84−1.01(m, 66H, Cy), −24.89 (td, J_{PH} = 17 Hz, J_{HH} = 8 Hz, 1H, Ir−H), −25.32(td, J_{PH} = 17 Hz, J_{HH} = 8 Hz, 1H, Ir−H). $^{31}P\{^1H\}$ NMR (202 MHz, CD_2Cl_2): δ 20.22 (s). $^{13}C\{^1H\}$ NMR (100 MHz, CD_2Cl_2): 128.70 (s), 121.90 (s), 100.88 (s), 36.94 (t, J = 13 Hz), 30.47 (s), 30.30 (s), 28.30 (t, J = 6 Hz), 27.39. (Not all carbon peaks were observed because of the low solubility). Anal. Calcd for $C_{47}H_{77}IrN_2P_2$: C, 61.07; H, 8.40; N, 3.03. Found: C, 59.94; H, 7.91; N, 2.71.

Dihydrido(2-amidopyrimidine-κ²-N,N′)bis(triphenylphosphine)-iridium(III) (6-PPh₃). To a suspension of $IrH_5(PPh_3)_2$ (117 mg, 0.16 mmol) in 10 mL of dry C_6H_6 in a 50-mL flame-dried Schlenk flask, 2-aminopyrimidine (19 mg, 0.20 mmol) was added. The mixture was heated at 70 °C for 20 h. The volatiles were removed under vacuum for 4 h. The resulting residue was redissolved in ∼1 mL of benzene and 1 mL of pentane was added. The resulting precipitate was decanted off the solution and washed with pentane and dried under vacuum to give **6-PPh₃** as an off-white solid. Yield: 92 mg, 70%. ^1H NMR (500 MHz, CD_2Cl_2): δ 7.62−7.58 (m, 12H, PPh_3), 7.36−7.28 (m, 18H, PPh_3), 7.42 (m, 1H, pyrimidine C−H), 7.06 (m, 1H, pyrimidine C−H), 6.72 (m, pyrimidine C−H), 3.89 (s, 1H, −NH), −22.21(td, J_{PH} = 20 Hz, J_{HH} = 10 Hz, 1H, Ir−H), −22.84 (m, 1H, Ir−H). $^{31}P\{^1H\}$ NMR (202 MHz, CD_2Cl_2): δ 19.31(t, J = 14 Hz). $^{13}C\{^1H\}$ NMR (126 MHz, CD_2Cl_2): δ 171.17 (s), 155.24 (s), 155.08 (s), 135.11 (t, J = 25 Hz), 134.03 (t, J = 6 Hz), 129.40 (s), 128.25 (s), 127.64 (t, J = 5 Hz), 102.09 (s). Anal. Calcd for $C_{40}H_{36}IrN_3P_2$: C, 59.10; H, 4.46; N, 5.17. Found: C, 60.12; H, 4.54; N, 4.85.

Trihydrido(pyridine)bis(triphenylphosphine)iridium(III) (8-PPh₃). To a suspension of $IrH_5(PPh_3)_2$ (70 mg, 0.10 mmol) in 10 mL of dry C_6H_6 in a 50-mL flame-dried Schlenk flask, pyridine (25 μL, 0.20 mmol) was added. The mixture was heated at 45 °C for 19 h. The volatiles were removed under vacuum for 4 h. The resulting residue was dissolved in ∼1 mL of benzene and 1 mL of pentane was added. The resulting precipitate was decanted off the solution and washed with pentane and dried under vacuum to give **8-PPh₃** as pale yellow solid. Yield: 51 mg, 63%. This compound has previously been prepared using an alternative method.[28] The IR spectrum of our sample matched that previously reported. The NMR data for **8-PPh₃** is reported here for future reference. ^1H NMR (500 MHz, C_6D_6): δ 8.36 (d, J = 6 Hz, 2H, pyridine C−H), 8.12−8.09 (m, 12H, PPh_3), 7.02−6.94 (m, 18H, PPh_3), 6.32 (m, 1H, pyridine C−H), 5.59 (dd, J = 7, 6 Hz, 2H, pyridine C−H), −8.73 (td, J_{PH} = 20 Hz, J_{HH} = 5 Hz, 2H, Ir−H), −21.98 (td, J_{PH} = 20 Hz, J_{HH} = 5 Hz, 1H, Ir−H). $^{31}P\{^1H\}$ NMR (202 MHz, C_6D_6): δ 33.50 (d, J = 16 Hz). $^{13}C\{^1H\}$ NMR (126 MHz,

C_6D_6): δ 160.77 (s), 138.50 (t, J = 25 Hz), 135.07 (t, J = 6 Hz), 128.83 (s), 128.59 (s), 127.57 (t, J = 4 Hz), 123.70 (s).

Dihydrido(N-(2-pyridyl)carbamato-κ²-N′,O)bis-(triphenylphosphine)iridium(III) (10-PPh₃). To a 25-mL round-bottomed flask was added trihydrido(2-aminopyridine)bis-(triphenylphosphine)iridium(III) (45.0 mg, 0.055 mmol) and DCM (3 mL). The flask was purged with CO_2 gas, which was bubbled through the solution for 10 min (alternatively the solution could be degassed using three freeze−pump−thaw cycles and then placed under a static atmosphere of CO_2). The reaction was allowed to stir for 24 h, during which time a white crystalline solid began to precipitate. The solid was filtered off under air, washed with DCM, cooled to 0 °C, and dried under vacuum. The precipitated crystals were suitable for X-ray diffraction. Yield 33.1 mg, 70%. ^{1}H NMR (500 MHz, CD_2Cl_2): δ 7.59 (m, 12H), 7.36 (d, J = 6.0 Hz, 1H), 7.27 (m, 18H), 6.93 (t, J = 7.8 Hz, 1H), 5.87 (d, J = 8.3 Hz, 1H), 5.68 (t, J = 6.0 Hz, 1H), δ −20.67 (td, J = 16.8, 7.1 Hz, 1H), −26.41 (td, J = 17.1, 7.4 Hz, 1H). ^{13}C{^{1}H} NMR: The full carbon spectrum of this compound could not be recorded due to its insolubility in all common solvents. ^{31}P{^{1}H} NMR (162 MHz, CD_2Cl_2): δ 21.30 (d, J = 15.3 Hz). IR (nujol, cm^{-1}): 1667.5 ($\nu_{C=O}$), 1329.1 ($\nu_{C=O}$). Anal. Calcd for $C_{42}H_{37}IrN_2O_2P_2$: C, 58.94; H, 4.36; N, 3.27. Found: C, 58.89; H, 4.31; N, 3.28.

An isotopologue of **10-PPh₃** with the carbon of the carbamato group ^{13}C-labeled was prepared by exposing a degassed solution of **10-PPh₃** in DCM to ^{13}C-labeled CO_2. Exchange occurred over a period of 24 h at RT. ^{13}C{^{1}H} NMR (126 MHz, CD_2Cl_2): 154.28 (^{13}C═O).

Dihydrido(N-(2-pyridyl)carbamato-κ²-N′,O)bis-(tricyclohexylphosphine)iridium(III) (10-PCy₃). Excess CO_2 at 1 atm was added via a dual-manifold Schlenk line to a degassed and shaken solution of **2-PCy₃** (6 mg, 0.007 mmol) in 0.8 mL of CD_2Cl_2 in a J. Young tube at RT. After 0.5 h the mixture was evaporated to dryness to give **10-PCy₃** as a white solid. Crystals suitable for X-ray diffraction were grown from CH_2Cl_2 at −35 °C. Yield: 5.8 mg, 92%. ^{1}H NMR (500 MHz, CD_2Cl_2): δ 8.42 (d, J = 5 Hz, 1H, pyridine C−H), 7.50 (br s, 1H, −NH), 7.43 (m, 1H, pyridine C−H), 6.46 (m, 2H, pyridine C−H), 1.96−1.05 (m, 66H, Cy), −23.64 (td, J_{PH} = 20 Hz, J_{HH} = 10 Hz, 1H, Ir−H), −28.83 (td, J_{PH} = 20 Hz, J_{HH} = 10 Hz, 1H, Ir−H). ^{31}P{^{1}H} NMR (202 MHz, CD_2Cl_2): δ 22.38. ^{13}C{^{1}H} NMR (126 MHz, CD_2Cl_2): δ 30.00 (s), 29.07 (s), 27.68 (br s), 26.80 (s), 26.30 (s). The full carbon spectrum of this compound could not be recorded due to its insolubility in all common solvents. IR (cm^{-1}) 1662 ($\nu_{C=O}$), 1311 ($\nu_{C=O}$). Anal. Calcd for $C_{42}H_{73}IrN_2O_2P_2{\cdot}CH_2Cl_2$: C, 52.85; H, 7.74; N, 2.87. Found: C, 52.44; H, 7.28; N, 2.84.

Dihydrido(N-(2-methylpyridyl)carbamato-κ²-N′,O)bis-(triphenylphosphine)iridium(III) (11-PPh₃). Excess CO_2 at 1 atm was added via a dual-manifold Schlenk line to a degassed and shaken solution of **4-PPh₃** (8.4 mg, 0.01 mmol) in 0.5 mL of CD_2Cl_2 in a J. Young tube at RT. After 0.5 h ^{1}H and ^{31}P spectra of the solution showed that it was a mixture containing 91% **10-PPh₃** and 9% **4-PPh₃**. The mixture was dried under vacuum for 2 h. ^{1}H and ^{31}P spectra of the resulting residue in CD_2Cl_2 showed that it was a mixture containing 27% **10-PPh₃** and 73% **4-PPh₃**. As a result no pure **10-PPh₃** was isolated. Crystals suitable for X-ray diffraction were grown from CH_2Cl_2/pentane under CO_2 at −35 °C. ^{1}H NMR (500 MHz, CD_2Cl_2): δ 7.69 (d, J = 5 Hz, 1H, pyridine C−H), 7.55−7.51 (m, 12H, Ar), 7.32−7.25 (m overlapping with **4-PPh₃**, 18H, Ar), 7.13 (m, 1H, pyridine C−H), 6.28 (d, J = 10 Hz, 1H, pyridine C−H), 5.83 (m, 1H, pyridine C−H), 2.38 (s, 3H, −NMe), −20.69 (m, 1H, Ir−H), −26.55 (m, 1H, Ir−H). ^{31}P{^{1}H} NMR (202 MHz, CD_2Cl_2): δ 20.22 (m).

Dihydrido(N-(2-pyrimidyl)carbamato-κ²-N′,O)bis-(triphenylphosphine)iridium(III) (12-PPh₃). Excess CO_2 at 1 atm was added via a dual-manifold Schlenk line to a degassed and shaken solution of **6-PPh₃** (28 mg, 0.034 mmol) in 1 mL of CH_2Cl_2 in a J. Young tube at RT. After 3 h the mixture was evaporated to dryness to give crude product. Pure **12-PPh₃** was obtained by recrystallization from CH_2Cl_2/pentane as a pale yellow solid. Yield: 19 mg, 65%. ^{1}H NMR (400 MHz, CD_2Cl_2): δ 7.89 (dd, J = 5, 2 Hz, 1H, pyrimidine C−H), 7.66 − 7.61 (m, 12H, PPh_3), 7.45−7.30 (m, 18H, PPh_3), 6.74 (s, 1H, pyrimidine C−H), 5.65 (m, pyrimidine C−H), −20.56 (td, J_{PH} = 16 Hz, J_{HH} = 8 Hz, 1H, Ir−H), −26.44 (td, J_{PH} = 16 Hz, J_{HH} = 8 Hz, 1H, Ir−H). ^{31}P{^{1}H} NMR (202 MHz, CD_2Cl_2): δ 21.93(m). ^{13}C{^{1}H} NMR (126 MHz, CD_2Cl_2): δ 165.03 (s), 158.35 (s), 157.31 (s), 153.68 (s), 134.46 (t, J = 6 Hz), 134.96(s), 133.96(s), 130.36, 128.85 (s), 128.58 (t, J = 5 Hz), 125.41(s), 113.43 (s). IR (cm^{-1}) 1674 ($\nu_{C=O}$), 1293 ($\nu_{C=O}$). Anal. Calcd for $C_{41}H_{36}IrN_3O_2P_2$: C, 57.47; H, 4.23; N, 4.90. Found: C, 56.10; H, 4.32; N, 4.85.

X-ray Crystallography. Crystal samples were mounted in MiTeGen polyimide loops with immersion oil. The diffraction experiments were carried out on a Rigaku SCXmini CCD detector using filtered MoKα radiation (λ = 0.71075 Å) at a temperature of −50 °C. The data frames were processed using Rigaku CrystalClear[29] and corrected for Lorentz and polarization effects. The structures were solved by direct methods[30] or Patterson methods[31] and expanded using Fourier techniques.[32] Non-hydrogen atoms were refined anisotropically and hydrogen atoms were typically treated as idealized contributions. Further details of the refinement are given in Table 2 and the Supporting Information.

Computational Details. All calculations were performed with the Gaussian09 package[33] of programs with the hybrid B3LYP functional.[34] The basis set was the ECP-adapted SDDALL[35] with a set of polarization functions for Ir[36] and P,[36] the all-electron 6-31G(d,p)[37] for N, H, C, and the 6-31+G(d,p)[38] for O of CO_2.[39] Full optimization of geometry was performed without any symmetry constraints, followed by analytical computation of the Hessian matrix to identify the nature of the located extrema as minima or transition states. Each transition state was relaxed toward reactant and product using the vibrational data to confirm its nature. The zero-point, thermal, and entropy corrections were evaluated to compute enthalpies and Gibbs free energies (T = 298 K, P = 1 atm). The effect of DCM solvent (ε = 8.93) was included by using the continuum SMD model[40] with single point 6-311+G** calculations.[41]

■ ASSOCIATED CONTENT

Supporting Information

Selected ^{1}H and ^{31}P NMR spectra, X-ray information for **1-PPh₃**, **2-PPh₃**, **3-PPh₃**, **7-PPh₃**, **10-PPh₃**, **10-PCy₃**, and **11-PPh₃**, the computed energy profile for the direct reaction of CO_2 with **1-PH₃**, the computed energy profile for the reaction between CO_2 and **2-PPh₃**, and Cartesian coordinates and energies for optimized structures. This material is available free of charge via the Internet at http://pubs.acs.org.

■ AUTHOR INFORMATION

Corresponding Author

*E-mail: robert.crabtree@yale.edu (R.H.C.), nilay.hazari@yale.edu (N.H.), anova@iciq.es (A.N.).

Notes

The authors declare no competing financial interest.

■ ACKNOWLEDGMENTS

G.E.D., N.D.S. and R.H.C. acknowledge funding from the Division of Chemical Sciences, Geosciences, and Biosciences, Office of Basic Energy Sciences of the U.S. Department of Energy through Grant DE-FG02-84ER13297. Financial support from the ICIQ foundation and the Spanish MICINN (projects CTQ2011-27033, Consolider Ingenio 2010 CSD2006-0003 and a Juan de la Cierva contract for A.N.) is acknowledged.

■ REFERENCES

(1) (a) Yu, K. M. K.; Curcic, I.; Gabriel, J.; Tsang, S. C. E. *ChemSusChem* **2008**, *1*, 893. (b) Riduan, S. N.; Zhang, Y. *Dalton Trans.* **2010**, *39*, 3347. (c) Darensbourg, D. J. *Inorg. Chem.* **2010**, *49*, 10765. (d) Cokoja, M.; Bruckmeier, C.; Rieger, B.; Herrmann, W. A.; Kühn, F. E. *Angew. Chem., Int. Ed.* **2011**, *50*, 8510. (e) Peters, M.; Köhler, B.; Kuckshinrichs, W.; Leitner, W.; Markewitz, P.; Müller, T. E. *ChemSusChem* **2011**, *4*, 1216.

(2) (a) Benson, E. E.; Kubiak, C. P.; Sathrum, A. J.; Smieja, J. M. *Chem. Soc. Rev.* **2009**, *38*, 89. (b) Rakowski DuBois, M.; DuBois, D. L. *Acc. Chem. Res.* **2009**, *42*, 1974.
(3) (a) Darensbourg, D. J. *Chem. Rev.* **2007**, *107*, 2388. (b) Sakakura, T.; Kohno, K. *Chem. Commun.* **2009**, 1312.
(4) (a) Jessop, P. G.; Ikariya, T.; Noyori, R. *Chem. Rev.* **1995**, *95*, 259. (b) Jessop, P. G.; Joo, F.; Tai, C.-C. *Coord. Chem. Rev.* **2004**, *248*, 2425. (c) Federsel, C.; Jackstell, R.; Beller, M. *Angew. Chem., Int. Ed.* **2010**, *49*, 6254.
(5) (a) Sakakura, T.; Choi, J.-C.; Yasuda, H. *Chem. Rev.* **2007**, *107*, 2365. (b) Hazari, N.; Hruszkewycz, D. P.; Wu, J. *Synlett* **2011**, *22*, 1793.
(6) Chaturvedi, D.; Ray, S. *Curr. Org. Chem.* **2007**, *11*, 987.
(7) Choi, S.; Drese, J. H.; Jones, C. W. *ChemSusChem* **2009**, *2*, 796.
(8) Behr, A. *Angew. Chem., Int. Ed.* **1988**, *27*, 661.
(9) Dell'Amico, D. B.; Calderazzo, F.; Labella, L.; Marchetti, F.; Pampaloni, G. *Chem. Rev.* **2003**, *103*, 3857.
(10) Hartwig, J. F.; Bergman, R. G.; Andersen, R. A. *J. Am. Chem. Soc.* **1991**, *113*, 6499.
(11) Park, S.; Rheingold, A. L.; Roundhill, D. M. *Organometallics* **1991**, *10*, 615.
(12) Schmeier, T. J.; Nova, A.; Hazari, N.; Maseras, F. *Chem.—Eur. J.* **2012**, *18*, 6915.
(13) Schmeier, T. J.; Dobereiner, G. E.; Crabtree, R. H.; Hazari, N. *J. Am. Chem. Soc.* **2011**, *133*, 9274.
(14) (a) Tanaka, R.; Yamashita, M.; Chung, L. W.; Morokuma, K.; Nozaki, K. *Organometallics* **2011**, *30*, 6742. (b) Tanaka, R.; Yamashita, M.; Nozaki, K. *J. Am. Chem. Soc.* **2009**, *131*, 14168. (c) Ahlquist, M. S. G. *J. Mol. Catal. A: Chem.* **2010**, *324*, 3. (d) Yang, X. *ACS Catal.* **2011**, *1*, 849.
(15) Lee, J. C.; Peris, E.; Rheingold, A. L.; Crabtree, R. H. *J. Am. Chem. Soc.* **1994**, *116*, 11014.
(16) Crabtree, R. H.; Demou, P. C.; Eden, D.; Mihelcic, J. M.; Parnell, C. A.; Quirk, J. M.; Morris, G. E. *J. Am. Chem. Soc.* **1982**, *104*, 6994.
(17) Crabtree, R. H.; Felkin, H.; Morris, G. E. *J. Organomet. Chem.* **1977**, *141*, 201.
(18) Deekan, S.; Motz, G.; Kempe, R. *Z. Anorg. Allg. Chem.* **2007**, *633*, 320.
(19) Park, S.; Lough, A. J.; Morris, R. H. *Inorg. Chem.* **1996**, *35*, 3001.
(20) Crabtree, R. H.; Morris, G. E. *J. Organomet. Chem.* **1977**, *135*, 395.
(21) Gruet, K.; Clot, E.; Eisenstein, O.; Lee, D. H.; Patel, B.; Macchioni, A.; Crabtree, R. H. *New J. Chem.* **2003**, *27*, 80.
(22) Peris, E.; Lee, J. C.; Rambo, J. R.; Eisenstein, O.; Crabtree, R. H. *J. Am. Chem. Soc.* **1995**, *117*, 3485.
(23) Crabtree, R. H.; Lavin, M. *J. Chem. Soc., Chem. Commun.* **1985**, 794.
(24) (a) Grotjahn, D. B.; Lo, H. C.; Groy, T. L. *Acta Crystallogr., Sect. C: Cryst. Struct. Commun* **1996**, *C52*, 516. (b) Grotjahn, D. B.; Lo, H. C.; Groy, T. L. *Acta Crystallogr., Sect. C: Cryst. Struct. Commun.* **1996**, *C52*, 300. (c) Fujita, K.-I.; Tanino, N.; Yamaguchi, R. *Org. Lett.* **2007**, *9*, 109. (d) Yamaguchi, R.; Ikeda, C.; Takahashi, Y.; Fujita, K.-I. *J. Am. Chem. Soc.* **2009**, *131*, 8410.
(25) Lee, D.-H.; Kwon, H. J.; Patel, B. P.; Liable-Sands, L. M.; Rheingold, A. L.; Crabtree, R. H. *Organometallics* **1999**, *18*, 1615.
(26) The mechanism of H_2 loss from **1-PPh$_3$** to form **2-PPh$_3$** will be addressed in a subsequent manuscript.
(27) Chisholm, M. H.; Extine, M. W. *J. Am. Chem. Soc.* **1977**, *99*, 792.
(28) Malatesta, L.; Caglio, G.; Angoletta, M. *J. Chem. Soc.* **1965**, 6974.
(29) *CrystalClear and CrystalStructure*; Rigaku/MSC: The Woodlands, TX, 2010.
(30) Altomare, A.; Cascarano, G.; Giacovazzo, C.; Guagliardi, A.; Burla, M. C.; Polidori, G.; Camalli, M. *J. Appl. Crystallogr.* **1994**, *27*, 435.
(31) Beurskens, P. T.; Beurskens, G.; de Gelder, R.; Garcia-Granda, S.; Gould, R. O.; Israel, R.; Smits, J. M. M. *The DIRDIF-99 Program System*; Crystallography Laboratory, University of Nijmegen: The Netherlands, 1999.
(32) Sheldrick, G. M. *Acta Crysallogr., A* **2008**, *64*, 112.
(33) Frisch, M. J.; Trucks, G. W.; Schlegel, H. B.; Scuseria, G. E.; Robb, M. A.; Cheeseman, J. R.; Scalmani, G.; Barone, V.; Mennucci, B.; Petersson, G. A.; Nakatsuji, H.; Caricato, M.; Li, X.; Hratchian, H. P.; Izmaylov, A. F.; Bloino, J.; Zheng, G.; Sonnenberg, J. L.; Hada, M.; Ehara, M.; Toyota, K.; Fukuda, R.; Hasegawa, J.; Ishida, M.; Nakajima, T.; Honda, Y.; Kitao, O.; Nakai, H.; Vreven, T.; Montgomery, Jr., J. A.; Peralta, J. E.; Ogliaro, F.; Bearpark, M.; Heyd, J. J.; Brothers, E.; Kudin, K. N.; Staroverov, V. N.; Kobayashi, R.; Normand, J.; Raghavachari, K.; Rendell, A.; Burant, J. C.; Iyengar, S. S.; Tomasi, J.; Cossi, M.; Rega, N.; Millam, N. J.; Klene, M.; Knox, J. E.; Cross, J. B.; Bakken, V.; Adamo, C.; Jaramillo, J.; Gomperts, R.; Stratmann, R. E.; Yazyev, O.; Austin, A. J.; Cammi, R.; Pomelli, C.; Ochterski, J. W.; Martin, R. L.; Morokuma, K.; Zakrzewski, V. G.; Voth, G. A.; Salvador, P.; Dannenberg, J. J.; Dapprich, S.; Daniels, A. D.; Farkas, Ö.; Foresman, J. B.; Ortiz, J. V.; Cioslowski, J.; Fox, D. J. *Gaussian 09, Revision A.02*; Gaussian, Inc.: Wallingford, CT, 2009.
(34) (a) Becke, A. D. *J. Chem. Phys.* **1993**, *98*, 5648. (b) Lee, C.; Parr, R. G.; Yang, W. *Phys. Rev. B.* **1988**, *37*, 785.
(35) (a) Andrae, D.; Haüssermann, U.; Dolg, M.; Stoll, H.; Preuss, H. *Theor. Chim. Acta.* **1990**, *77*, 123. (b) Bergner, A.; Dolg, M.; Küchle, W.; Stoll, H.; Preuss, H. *Mol. Phys.* **1993**, *80*, 1431.
(36) Höllwarth, A.; Böhme, H.; Dapprich, S.; Ehlers, A. W.; Gobbi, A.; Jonas, V.; Köhler, K. F.; Stegmann, R.; Veldkamp, A.; Frenking, G. *Chem. Phys. Lett.* **1993**, *203*, 237.
(37) Hariharan, P. C.; Pople, J. A. *Theor. Chim. Acta.* **1973**, *28*, 213.
(38) Frisch, M. J.; Pople, J. A.; Binkley, J. S. *J. Chem. Phys.* **1984**, *80*, 3265.
(39) The inclusion of diffuse functions is recommended in those cases where negative charge is located on one atom. In this study, the use of diffuse functions for oxygen was essential to locate the stepwise mechanism obtained for the insertion of CO_2 into **2-PH$_3$**.
(40) Marenich, A. V.; Cramer, C. J.; Truhlar, D. G. *J. Phys. Chem. B* **2009**, *113*, 6378.
(41) (a) Balcells, D.; Ujaque, G.; Fernandez, I.; Khiar, N.; Maseras, F. *J. Org. Chem.* **2006**, *71*, 6388. (b) Braga, A. A. C.; Ujaque, G.; Maseras, F. *Organometallics* **2006**, *25*, 3647.